Rapid Eocene erosion, sedimentation and burial in the eastern Himalayan syntaxis and its geodynamic significance

Journal Item

Gondwana Research xxx (2012) xxx–xxx

Contents lists available at SciVerse ScienceDirect

Gondwana Research

journal homepage: www.elsevier.com/locate/gr

Rapid Eocene erosion, sedimentation and burial in the eastern Himalayan syntaxis and its geodynamic significance

Wang-Chun Xu [a,*], Hong-Fei Zhang [a,*], Nigel Harris [b], Liang Guo [a], Fa-Bing Pan [a]

[a] State Key Laboratory of Geological Processes and Mineral Resources, Faculty of Earth Sciences, China University of Geosciences, Wuhan 430074, PR China
[b] Department of Environment, Earth and Ecosystems, The Open University, Milton Keynes, MK7 6AA, UK

ARTICLE INFO

Article history:
Received 19 January 2012
Received in revised form 28 April 2012
Accepted 11 May 2012
Available online xxxx

Handling Editor: Z. Zhang

Keywords:
Zircon U–Pb geochronology
Lower Bomi Group
Geodynamics
The eastern Himalayan syntaxis
Lhasa terrane

ABSTRACT

The lower Bomi Group of the eastern Himalayan syntaxis comprises a lithological package of sedimentary and igneous rocks that have been metamorphosed to upper amphibolite-facies conditions. The lower Bomi Group is bounded to the south by the Indus–Yarlung Suture and to the north by unmetamorphosed Paleozoic sediments of the Lhasa terrane. We report U–Pb zircon dating, geochemistry and petrography of gneiss, migmatite, mica schist and marble from the lower Bomi Group and explore their geological implications for the tectonic evolution of the eastern Himalaya. Zircons from the lower Bomi Group are composite. The inherited magmatic zircon cores display $^{206}Pb/^{238}U$ ages from ~74 Ma to ~41.5 Ma, indicating a probable source from the Gangdese magmatic arc. The metamorphic overgrowth zircons yielded $^{206}Pb/^{238}U$ ages ranging from ~38 Ma to ~23 Ma, that overlap the anatexis time (~37 Ma) recorded in the leucosome of the migmatites. Our data indicate that the lower Bomi Group do not represent Precambrian basement of the Lhasa terrane. Instead, the lower Bomi Group may represent sedimentary and igneous rocks of the residual forearc basin, similar to the Tsojiangding Group in the Xigaze area, derived from denudation of the hanging wall rocks during the India–Asia continental collision. We propose that following the Indian–Asian collision, the forearc basin was subducted, together with Himalayan lithologies from the Indian continental slab. The minimum age of detrital magmatic zircons from the supracrustal rocks is ~41.5 Ma and their metamorphism had happened at ~37 Ma. The short time interval (<5 Ma) suggests that the tectonic processes associated with the eastern Himalayan syntaxis, encompassing uplift and erosion of the Gangdese terrane, followed by deposition, imbrication and subduction of the forearc basin, were extremely rapid during the Late Eocene.

1. Introduction

Many studies have demonstrated that continental crust can be subducted to depths in excess of at least 80 km, possibly to depths of 200 to 350 km (Xu et al., 1992; Yang et al., 1993; Dobrzhinetskaya et al., 1996; Bozhilov et al., 1999; Ye et al., 2000; Zheng, 2003; Liu et al., 2007a, 2008a). During the deep subduction, continental crust underwent high-pressure (HP) to ultrahigh-pressure (UHP) metamorphism and resulted in the formation of various HP and UHP metamorphic rocks in the orogen. Because of the buoyancy of felsic continental crust, exhumation of deeply subducted continental crust is hypothesized to follow slab breakoff that occurs at the transition zone between the continental and oceanic lithosphere (Zheng et al., 2009). These exhumed rocks provide an insight into the subduction of continental crust.

The Indian continent has been subducted under the Eurasian continent, forming the Himalayan–Tibetan orogen, one of the youngest and most spectacular orogens on Earth (Yin and Harrison, 2000). To better understand the Indian continental subduction, investigations that were carried out over recent decades have focused largely on the Himalayan metamorphic and magmatic rocks of the Indian plate that form the footwall of the subduction zone (Tonarini et al., 1993; Guillot et al., 1997; de Sigoyer et al., 2000; Ding et al., 2001; O'Brien et al., 2001; Kaneko et al., 2003; Mukherjee et al., 2003; Leech et al., 2005; Parrish et al., 2006; Liu et al., 2007b; Guillot et al., 2008; Booth et al., 2009; Cottle et al., 2009; Xu et al., 2010). The hanging wall of the subduction zone, known as the southern Lhasa terrane, is dominated by Jurassic–Paleocene magmatic rocks related to the tectono-thermal evolution of an Andean-type arc (Mo et al., 2003; Chu et al., 2006; Mo et al., 2007; Mo et al., 2008; Wen et al., 2008; Chiu et al., 2009; Ji et al., 2009; Chu et al., 2011; Xia et al., 2011; Zhu et al., 2011b, 2012; Guan et al., 2012). In the southern Lhasa, studies of the metamorphic assemblages are comparatively sparse (Harris et al., 1988; Li et al., 2009; Yang et al., 2009; Dong et al., 2010, 2011; Zhang et al., 2010b).

In the eastern Himalayan syntaxis (EHS), high-grade metamorphic rocks (Bomi Group) are well exposed by rapid uplift and erosion (Burg et al., 1997). The Bomi Group consists of gneiss, migmatite, mica schist, amphibolite and marble. The Bomi Group was previously

* Corresponding authors. Tel.: +86 27 67883003; fax: +86 27 67883002.
E-mail address: hfzhang@cug.edu.cn (H.-F. Zhang).

1342-937X/$ – see front matter © 2012 International Association for Gondwana Research. Published by Elsevier B.V. All rights reserved.
doi:10.1016/j.gr.2012.05.011

considered to be Precambrian, representing crustal basement of the southern Lhasa terrane in the EHS (Li, 1955; Dewey et al., 1988; Zheng et al., 2003). In this study, we carried out U–Pb zircon dating for the mica schist, marble and gneiss and undeformed leucosome from the lower Bomi Group. Our data show that the protolith of the lower Bomi Group formed during the Early Paleogene, and has experienced significant metamorphism during the Eocene–Miocene. Our data provide new constraints on the geological history of the lower Bomi Group and explores their tectonic implications for Indian continental subduction.

2. Geological setting and sample description

2.1. Regional geology

The eastern Himalayan syntaxis is the eastern termination of the Himalaya collisional orogen (Fig. 1). The main structural fabric and lithological features of the Himalaya limit an uplifted area at Namche Barwa and coincide with the 'U-turn' of the Yalu-Tsangpo River (Burg et al., 1998; Zeitler et al., 2001). The EHS comprises three major tectono-stratigraphic units (Geng et al., 2006): (1) the Namche Barwa Group of the Himalayan unit; (2) the Indus–Yarlung Suture unit (IYS); and (3) the Gangdese unit. The northwestern and southeastern contacts between the Namche Barwa Group and the Gangdese unit are marked by the sinistral Dongjiu–Miling Fault and dextral Aniqiao Fault, respectively. The syntaxis is cut at its northeastern tip by the active dextral Jiali–Parlung Fault (Burg et al., 1997, 1998; Zhang et al., 2004).

The Namche Barwa Group, the core of the EHS, includes layered felsic gneisses that were locally migmatized (Burg et al., 1998). According to recent geological mapping (Geng et al., 2006), the Namche Barwa Group can be subdivided into three subunits: Zhibai Formation, Duoxiongla Complex and Paixiang Formation, separated by ductile faults (Xu et al., 2008, 2012). The Zhibai Formation comprises garnet-bearing gneisses containing sporadic boudins of HP granulite, with peak metamorphic temperature–pressure conditions estimated at ~850 °C and 14–18 kbar (Zhong and Ding, 1996; Liu and Zhong, 1997; Ding and Zhong, 1999; Geng et al., 2006; Booth et al., 2009). The age of peak metamorphism for the HP granulites has been variably estimated from ~40 Ma to ~24 Ma (Ding et al., 2001; Liu et al., 2007b; Xu et al., 2010; Zhang et al., 2010b; Su et al., 2012). The Duoxiongla Complex comprises migmatitic gneisses and orthogneisses with protolith ages ranging from 1.6 Ga to 1.8 Ga, as determined by U–Pb zircon dating (Guo et al., 2008; Zhang et al., 2012). The Paixiang Formation is composed of felsic gneisses with subordinate diopside and forsterite-bearing marbles (Geng et al., 2006). The Namche Barwa Group is intruded by Neogene granitoids with ages of ~13–3 Ma (Burg et al., 1998; Ding et al., 2001; Booth et al., 2004).

The IYS unit separates the Himalaya unit (Namche Barwa Group in the Indian plate) to the south from the Gangdese unit (Lhasa terrane in the Asian plate) to the north (Fig. 1). It is a continuous zone, 2–10 km wide, consisting of highly deformed and metamorphosed sedimentary and ultramafic–mafic rocks, the latter representing a Neo-Tethyan ophiolite (Geng et al., 2006). In the EHS, the geochemistry of the IYS mafic rocks indicate a back-arc basin affinity (Geng et al., 2006), comparable to mafic rocks that crop out to the west at Xigaze and Zedang regions. Clinopyroxene $^{40}Ar/^{39}Ar$ dating for the IYS mafic rocks yielded a crystallization age of 200 ± 4 Ma (Geng et al., 2004).

The Gangdese unit includes the Nyingchi Group, the Bomi Group, Paleozoic–Mesozoic cover strata, and abundant Mesozoic–Cenozoic granites (Fig. 1). The Nyingchi Group comprises gneisses, schists, marbles and minor granulites. These rocks have experienced upper amphibolite-facies metamorphism, locally rising to granulite grade (Zhang et al., 2010b,c). Detrital zircon age data suggest that the maximum depositional age of the Nyingchi Group is no older than 490 Ma (Zhang et al., 2008; Dong et al., 2010). The Bomi Group is exposed over the northern and eastern margin of the EHS. It can be divided into three subunits (Zheng et al., 2003): (1) the lower Bomi Group with gneisses, migmatites, schists, amphibolites and minor marbles; (2) the middle Bomi Group that consists of gneisses, migmatites and amphibolites; and (3) the upper Bomi Group that is dominated by gneisses. The metamorphic P–T condition for the Bomi Group was estimated at 3–8 kbar and 575–640 °C (XBGMR, 1995; Zheng et al., 2003) or at ~10.8 kbar and ~840 °C (Booth et al., 2009). The Bomi Group has been interpreted to represent the Precambrian metamorphic basement of the Lhasa terrane (Li, 1955; Dewey et al., 1988; Zheng et al., 2003). The Gangdese unit granites were mostly emplaced during two intrusive episodes, at ~133–110 Ma and at ~66–57 Ma (Booth et al., 2004, 2009; Chiu et al., 2009; Zhang et al., 2010a; Guo et al., 2012). Chiu et al. (2009) suggested that the early Cretaceous granites were probably formed in a post-collisional regime

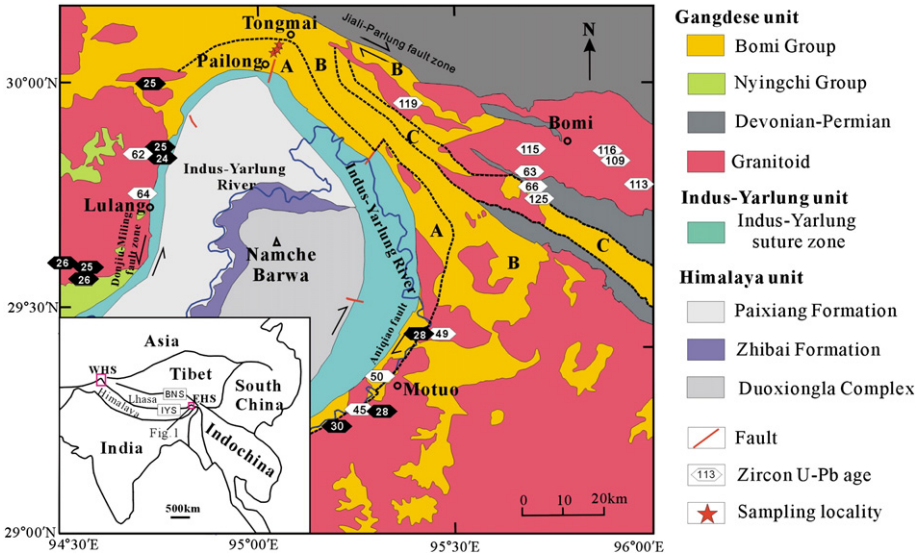

Fig. 1. Sketch map of the eastern Himalayan syntaxis, showing sample location (modified after Zheng et al. (2003)). Inset denotes the location of study area in southern Asia. Abbreviations: A = lower Bomi Group; B = middle Bomi Group; C = upper Bomi Group; BNS = Bangong–Nujiang Suture zone; IYS = Indus–Yarlung Suture zone; WHS = the western Himalayan syntaxis; and EHS = the eastern Himalayan syntaxis.
Zircon U–Pb ages are from Chung et al. (2003), Booth et al. (2004), Zhang et al. (2008), Chiu et al. (2009), and our unpublished data.

Please cite this article as: Xu, W.-C., et al., Rapid Eocene erosion, sedimentation and burial in the eastern Himalayan syntaxis and its geodynamic significance, Gondwana Res. (2012), doi:10.1016/j.gr.2012.05.011

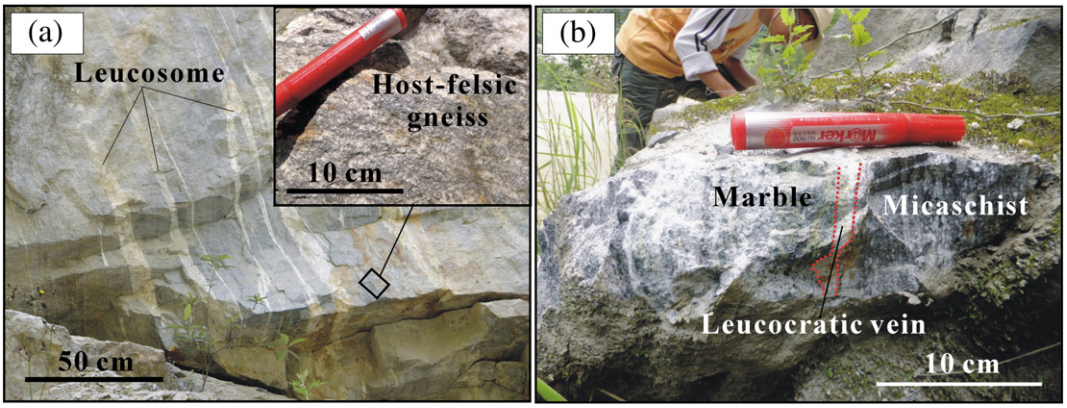

Fig. 2. Field photographs showing the occurrences of the lower Bomi Group in the eastern Himalayan syntaxis. (a) Leucosome and its host-felsic gneiss; (b) mica schist and marble.

in response to the Late Jurassic–Early Cretaceous collision between the Qiangtang and Lhasa terrane. The Late Cretaceous–Paleocene granites resulted from northward subduction of the Neo-Tethys during late Mesozoic time (Chiu et al., 2009; Zhang et al., 2010c; Guo et al., 2011). The Cretaceous–Paleocene granites were intruded by the later muscovite granite, two-mica granite and garnet granite, ranging from ~26–21 Ma in age (Ding et al., 2001; Chung et al., 2003; Booth et al., 2004; Zhang et al., 2008, 2010a; Guo et al., 2011). These Late Oligocene–Early Miocene granites resulted from partial melting of thickened lower crust (Chung et al., 2003; Booth et al., 2004).

2.2. Sample description

The lower Bomi Group is well exposed in the northern margin of the EHS (Fig. 1) as seen on the road from Pailong to Tongmai. Our field observation shows that the mica schists in the EHS occur as layers ranging from several meters to several tens of meters in thickness, whereas marbles occur as thin layers or lenses (Fig. 2b). The mica schists are foliated, as defined by aligned biotite, amphibole and muscovite. The migmatite consists of ~70% mesosome (gray felsic gneisses) and ~30% garnet-bearing leucosome (Fig. 2a). Aligned biotite flakes in the felsic gneisses define the foliation, which is parallel to the foliation of the mica schist. The leucosomes are typically <10 cm in thickness and tend to form sub-parallel arrays, which are consistent with the foliation orientation of the felsic gneisses. The contact between the migmatite and mica schist is not observed. The gneiss sample T824 is composed of plagioclase (~25%), K-feldspar (~40%), quartz (~25%), biotite (~7%), and muscovite (~2%), with minor amounts of zircon and Fe–Ti oxides (Fig. 3d). The leucosome sample T823, collected from the same outcrop as former sample, is composed of plagioclase (~30%), quartz (~50%), garnet (~15%), muscovite and biotite (~4%) and accessory zircon and Fe–Ti oxides (Fig. 3c). Two further samples were collected from the neighboring outcrop; a garnet–mica schist (sample T818) and a marble (sample T819). The schist sample T818 consists mainly of plagioclase (~50%), quartz (~16%), biotite (~15%), amphibole (~12%), garnet

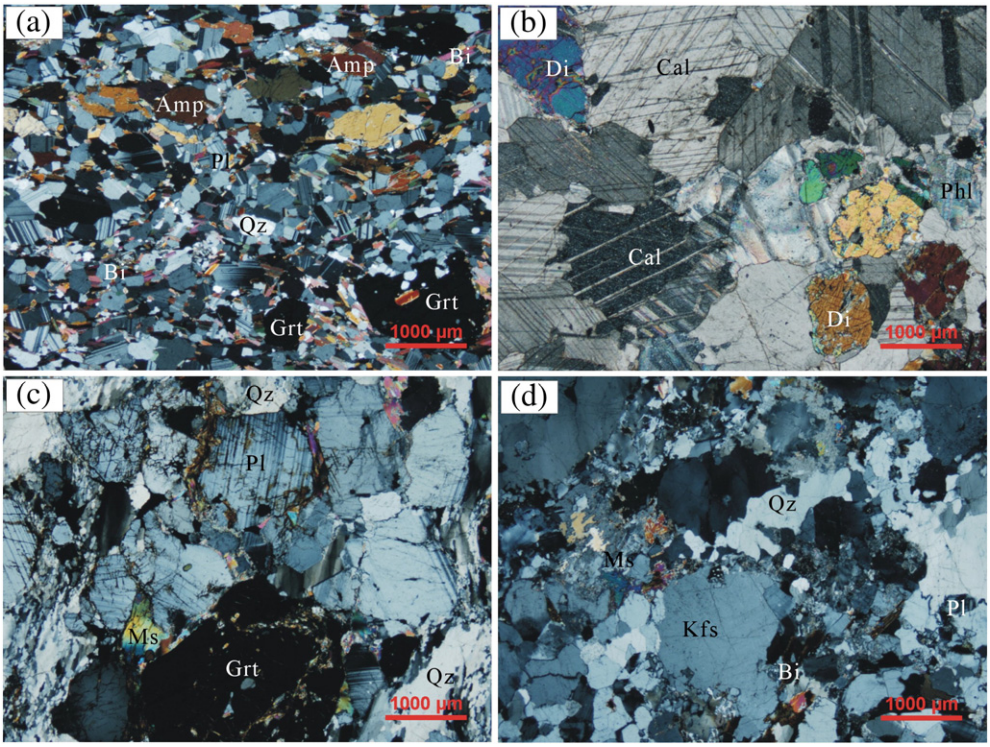

Fig. 3. Microstructures of (a) the garnet-mica schist sample T818, (b) the marble sample T819, (c) the leucosome sample T823 and (d) the felsic gneiss sample T824. Amp = amphibole, Bi = biotite, Cal = calcite, Di = diopside, Grt = garnet, Kfs = K-feldspar, Ms = muscovite, Phl = phlogopite, Pl = plagioclase, and Qz = quartz.

Please cite this article as: Xu, W.-C., et al., Rapid Eocene erosion, sedimentation and burial in the eastern Himalayan syntaxis and its geodynamic significance, Gondwana Res. (2012), doi:10.1016/j.gr.2012.05.011

(~5%), muscovite (~1%), and accessory minerals including zircon, apatite, epidote, and Fe–Ti oxides (Fig. 3a). In thin-section, sample T818 typically has a layered appearance with a layer width of 3–10 mm. Some layers are dominantly composed of amphibole and plagioclase; some layers are largely made up of biotite and plagioclase whereas others consist of quartzofeldspathic minerals. The varying modal compositions between layers could indicate contrasting chemical compositions in the protolith, presumably emphasized by metamorphic differentiation. The marbles form layers that are sandwiched within or between the mica schists and the gneisses. The marble sample T819 is composed of calcite (~88%), diopside (~6%), phlogopite (~3%), and quartz (~2%) (Fig. 3b), with accessory minerals of apatite and zircon.

Petrographic observations show that the mica schists from the lower Bomi Group share a similar mineral paragenesis, characterized by the assemblage plagioclase + amphibole + biotite + garnet + quartz + muscovite, indicating amphibolite-facies metamorphic conditions. The mineral assemblage of calcite + diopside + phlogopite + quartz in the marble also provides an indication of amphibolite-facies metamorphism. P–T estimation for the lower Bomi Group gave peak-metamorphic conditions at T = 575–640 °C and P = 3–8 kbar (XBGMR, 1995; Zheng et al., 2003).

3. Analytical methods

Zircons were separated by heavy-liquid and magnetic methods and then purified by hand picking under a binocular microscope. Zircon crystals were mounted in an epoxy disk and then were polished. Cathodoluminescence (CL) imaging was carried out at the State Key Laboratory of Continental Dynamics, Northwest University, Xi'an, China. Zircons were selected and analyzed synchronously for trace-element contents and isotopic compositions using LA-ICP-MS at the State Key Laboratory of Geological Processes and Mineral Resources, China University of Geosciences, Wuhan, China. Detailed operating conditions for the laser ablation system and the ICP-MS instrument and data reduction are the same as description by Liu et al. (2008b, 2010a,b). Laser sampling was performed using a GeoLas 2005. An Agilent 7500a ICP-MS instrument was used to acquire ion-signal intensities. The laser spot is 32 μm in diameter. Helium was applied as a carrier gas. Argon was used as the make-up gas and mixed with the carrier gas via a T-connector before entering the ICP. Nitrogen was added into the central gas flow (Ar + He) of the Ar plasma to decrease the detection limit and improve precision (Hu et al., 2008). Each analysis incorporated a background acquisition of approximately 20–30 s (gas blank) followed by 50 s data acquisition from the sample. The Agilent Chemstation was utilized for the acquisition of each individual analysis. Off-line selection and integration of background and analyte signals, and time-drift correction and quantitative calibration for trace element analyses and U–Pb dating were performed by *ICPMSDataCal* (Liu et al., 2008b, 2010a).

Zircon 91500 was used as external standard for U–Pb dating, and was analyzed twice every 5 analyses. Time-dependent drifts of U–Th–Pb isotopic ratios were corrected using a linear interpolation (with time) for every 5 analyses according to the variations of 91500 (i.e., 2 zircon 91500 + 5 samples + 2 zircon 91500) (Liu et al., 2010a). Preferred U–Th–Pb isotopic ratios used for 91500 are from Wiedenbeck et al. (1995). The uncertainty of preferred values for the external standard 91500 was propagated to the ultimate results of the samples. The common Pb correction is computed by the EXCEL program of ComPbCorr#3-151 (Andersen, 2002), assuming that the observed $^{206}Pb/^{238}U$, $^{207}Pb/^{235}U$ and $^{208}Pb/^{232}Th$ ratios for a discordant zircon can be accounted for by a combination of lead loss at a defined time. Concordia diagrams and weighted mean calculations were made using Isoplot/Ex_ver3 (Ludwig, 2003). Trace-element compositions of zircons were calibrated against multiple-reference materials (BCR-2G, BIR-1G and GSE-1G) combined with internal standardization (Liu et al., 2010a). The preferred values of element concentrations for the USGS reference glasses are from the GeoReM database (http://georem.mpch-mainz.gwdg.de/).

4. Results

4.1. Zircon U–Pb geochronology and trace elements

Representative zircon CL images, U–Pb Concordia plots and chondrite-normalized REE pattern for zircons are shown in Figs. 4, 5 and 6, respectively. LA-ICP-MS zircon U–Pb and trace-elements data are listed in the supplemental electronic data tables (Tables A and B). The errors for individual U–Pb analyses are given in 1σ and uncertainties in Concordia diagrams are quoted at 95% level (2σ).

4.1.1. Garnet–mica schist

Most zircons from sample T818 are euhedral prismatic grains, 120–300 μm in length, with large length-to-width ratios ranging from 5:1 to 10:1, which suggest rapid crystallization in volcanic rocks (Hoskin and Schaltegger, 2003). CL images reveal that these grains are composite with an oscillatory zoned core, surrounded by a weakly luminescent unzoned rim (Fig. 4a). The boundary between the core and rim is rounded, straight or embayed, suggesting possible resorption and recrystallization (Corfu et al., 2003). Both the zircon morphology and internal structure suggest that the cores are magmatic and the rims are metamorphic in origin (Vavra et al., 1996, 1999; Corfu et al., 2003).

Fifty-eight analyses on zircon cores from sample T818 yielded $^{206}Pb/^{238}U$ ages of 63.0–46.8 Ma, with a dominant cluster of $^{206}Pb/^{238}U$ ages at ~58 Ma. Eight analyses on zircon rims gave $^{206}Pb/^{238}U$ ages of 38–28 Ma (Fig. 5a). The cores have U of 114–3633 ppm, Th of 49.2–2236 ppm and Th/U values of 0.26–1.53. The rims have U of 244–1827 ppm, Th of 28.8–172 ppm and Th/U ratios of 0.03–0.21 (excepting a single Th/U of 0.74). The low Th/U ratios for the rims are consistent with a metamorphic origin (Rubatto, 2002). Both the cores and rims have steep chondrite-normalized REE patterns with pronounced positive Ce anomalies and negative Eu anomalies (Fig. 6a). The rims show lower HREE contents than the cores, reflecting the synchronously crystallization of garnet during formation of the zircon rims. This is consistent with the occurrence of garnet in the host rock (Fig. 3a).

4.1.2. Marble

Most zircons from marble sample T819 are prismatic crystals of variable length, but generally have rounded terminations. They have grain sizes of 50–150 μm in length, with ratios of length to width ranging from 1:1 to 4:1. Their CL images (Fig. 4b) exhibit complex core and rim structures. The cores are commonly angular with oscillatory zoning and resorption, interpreted as inherited magmatic zircons (Corfu et al., 2003). The weakly luminescent rims are unzoned, implying that they are metamorphic (Vavra et al., 1996, 1999; Corfu et al., 2003). The contacts between the luminescent cores and the weakly luminescent rims are angular, sharp, and cut across the zonation patterns in the cores (Fig. 4b).

Twenty-seven zircon cores were dated. They are concordant and near-concordant, and yielded $^{206}Pb/^{238}U$ ages of 62.0–41.5 Ma (Fig. 5b). The cores have U of 136–9777 ppm, Th of 103–3013 ppm and Th/U values of 0.19–0.94. Fourteen analyses on zircon rims gave $^{206}Pb/^{238}U$ ages of 37.4–23.7 Ma. The rims have U of 247–5739 ppm, Th of 10.4–610 ppm and Th/U ratios of 0.01–0.36. Both the cores and rims show enrichment in HREE, a positive Ce anomaly and a negative Eu anomaly, except for a few egregious analyses (Fig. 6b). Rims show much steeper HREE patterns than do the cores.

4.1.3. Leucosome

Zircons from leucosome sample T823 are short prismatic crystals, 100–150 μm in length, with ratios of length to width ranging from 2:1

Please cite this article as: Xu, W.-C., et al., Rapid Eocene erosion, sedimentation and burial in the eastern Himalayan syntaxis and its geodynamic significance, Gondwana Res. (2012), doi:10.1016/j.gr.2012.05.011

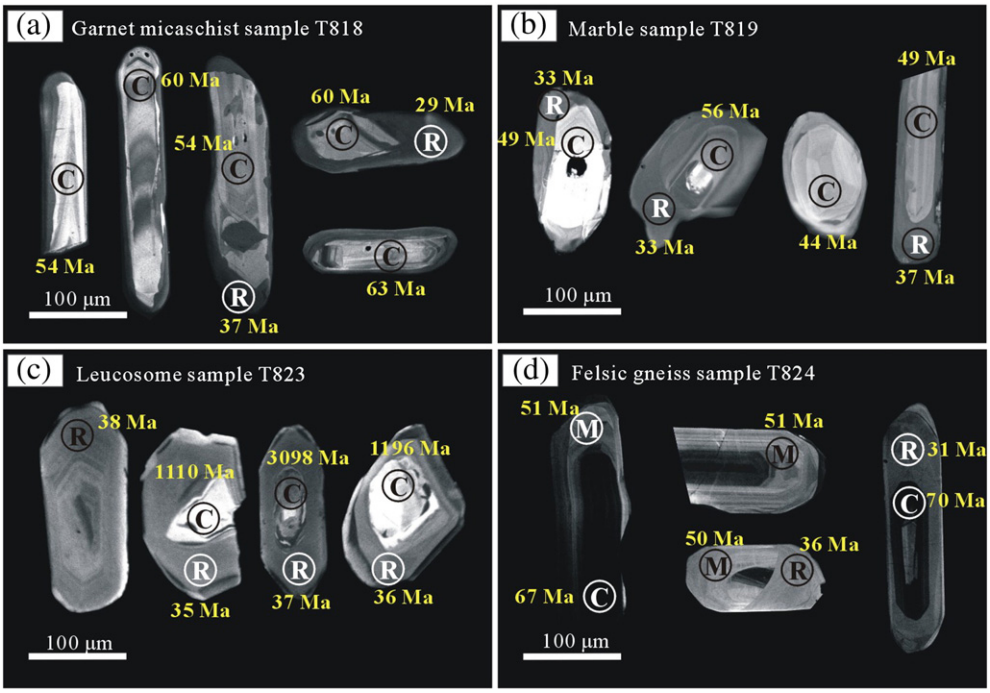

Fig. 4. Representative cathodoluminescence images of zircons from (a) the garnet-mica schist sample T818, (b) the marble sample T819, (c) the leucosome sample T823, and (d) the felsic gneiss sample T824. The circles show LA-ICP-MS dating spots and corresponding apparent ages. C = core, M = mantle, and R = rim.

to 3:1. In CL images, zircons commonly show complicated core–rim structures. The cores are rounded or subrounded and are unzoned with relatively strong luminescence brightness (Fig. 4c). The rims display great variation in their thickness and internal structure. Some rims, characterized by oscillatory zoning, are suggestive of magmatic zircon (Corfu et al., 2003). However, other rims exhibit

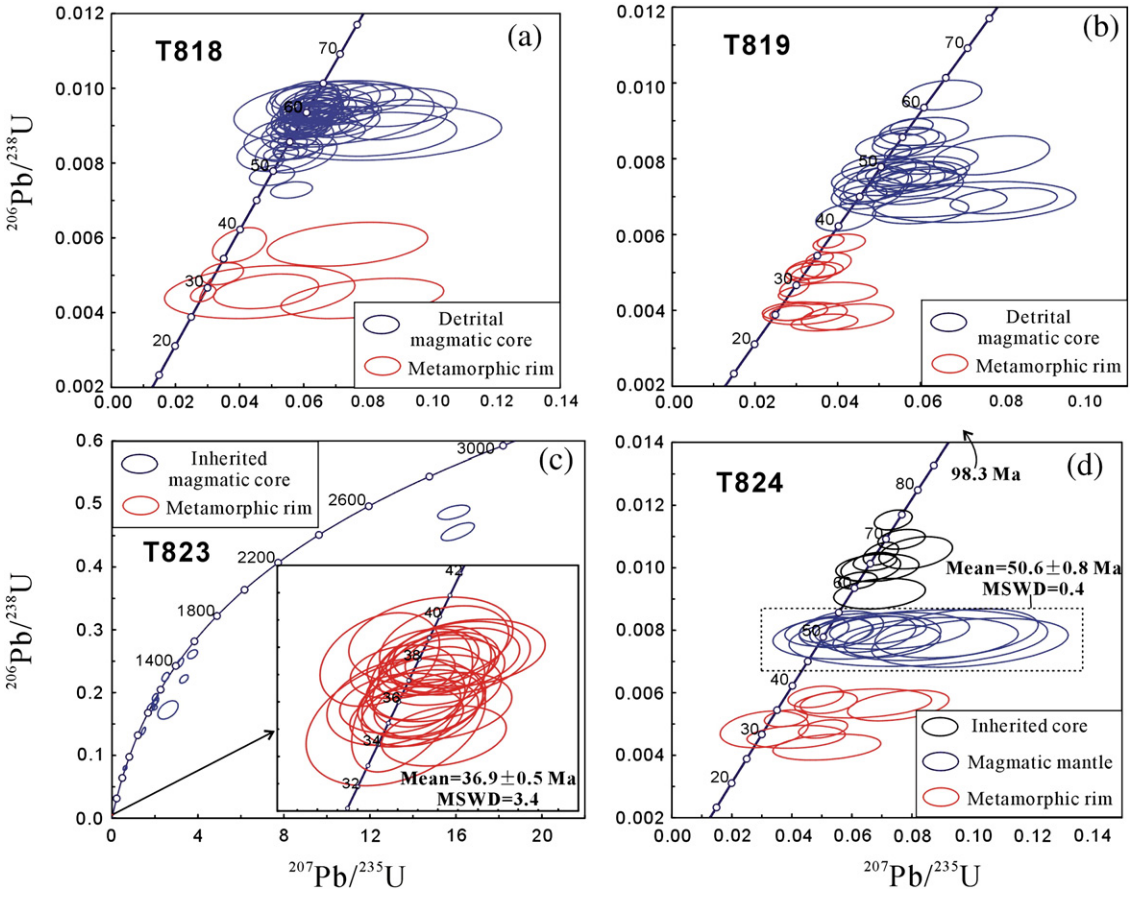

Fig. 5. Concordia diagrams of LA-ICP-MS U–Pb dating for zircons from (a) garnet-mica schist sample T818, (b) marble sample T819, (c) leucosome sample T823 and (d) felsic gneiss sample T824.

Please cite this article as: Xu, W.-C., et al., Rapid Eocene erosion, sedimentation and burial in the eastern Himalayan syntaxis and its geodynamic significance, Gondwana Res. (2012), doi:10.1016/j.gr.2012.05.011

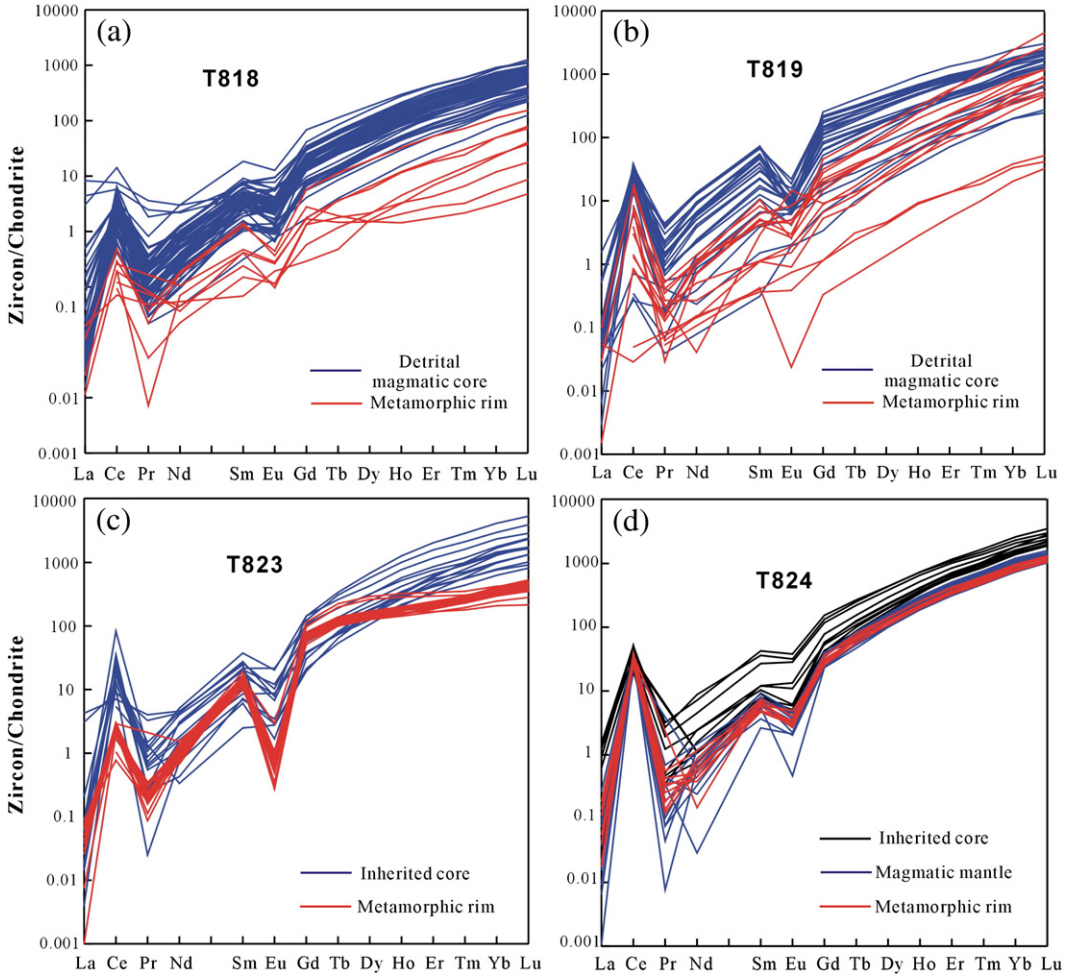

Fig. 6. Chondrite-normalized REE patterns for zircons from the metamorphic rocks in the lower Bomi Group. (a) The sample T818, (b) the sample T819, (c) the sample T823 and (d) the sample T824.
Normalizing values are from Boyton (1984).

planar or no zoning (Fig. 4c). These characteristics of the zircon rims have been observed in zircons crystallizing from an anatectic melt (Wu and Zheng, 2004). In addition, many zircons exhibit an extremely narrow (<5 μm) outer rim with high CL intensity. It may represent later thermal activity but their narrow width has precluded precise dating.

Twenty-five analyses of zircon rims define a cluster of $^{206}Pb/^{238}U$ ages with a weighted mean of 36.9 ± 0.5 Ma (2σ; MSWD = 3.4) (Fig. 5c), which is considered as the timing of anatexis. They have U of 680–1516 ppm, Th of 48–143 ppm and Th/U of 0.03–0.16. The low Th/U ratios for the rims are consistent with a metamorphic origin (Rubatto, 2002). Fifteen analyses were undertaken on the inherited zircon cores. They gave variable U–Pb ages of 171–3211 Ma, with a peak at ~1180 Ma (Fig. 7f). They have U of 13.1–3414 ppm, Th of 10.9–1452 ppm and Th/U of 0.03–1.50. The cores have steep chondrite-normalized REE patterns with both pronounced positive Ce anomalies and negative Eu anomalies (Fig. 6c). In contrast, the rims have strikingly lower HREE contents than the cores, and show flat HREE patterns, which indicate the simultaneous crystallization of garnet during formation of the zircon rims. This is supported by the presence of garnet in the host rock (Fig. 3c).

4.1.4. Felsic gneiss

Most zircons from gneiss sample T824 show short to long prismatic crystals, but generally have rounded terminations. They have grain sizes of 100–200 μm in length, with ratios of length to width ranging from 1:1 to 5:1. In CL images, they commonly show complicated core–mantle–rim structures (Fig. 4d). The cores are subrounded with oscillatory zoning showing relatively weak luminescence, whereas the mantles exhibit oscillatory zoning with strong luminescence (Fig. 4d). Both core and mantle appear to be magmatic in origin (Corfu et al., 2003). The rims, however, exhibit planar zoning or no zoning (Fig. 4d), which is typical of a metamorphic origin (Vavra et al., 1996, 1999; Corfu et al., 2003). The boundaries between the oscillatory and planar or unzoned domains are often blurred, implying that the metamorphic rims are probably produced by the later thermal alteration.

Twelve zircon mantle analyses show consistent $^{206}Pb/^{238}U$ ages, with a weighted mean $^{206}Pb/^{238}U$ age of 50.6 ± 0.8 Ma (2σ; MSWD = 0.4), representing the magma crystallization age. Nine rim analyses yielded $^{206}Pb/^{238}U$ ages of 37.7–27.0 Ma (Fig. 5d). Ten cores were dated, of which one analysis has a $^{206}Pb/^{238}U$ age of 98.3 Ma and the remaining analyses yielded $^{206}Pb/^{238}U$ ages ranging from 73.9 ± 0.8 Ma to 59.0 ± 1.0 Ma (Fig. 5d). The mantles and rims show similar U and Th compositions. Both have U of 207–517 ppm, Th of 131–247 ppm and Th/U ratios of 0.37–0.72. The cores have higher U (650–1997 ppm) and Th (219–969 ppm) contents than the mantles and rims, but their Th/U ratios (0.24–0.81) are not distinct from the mantles and rims. All the core–mantle–rims have similar REE compositions, characterized by enrichment in HREE, a positive Ce anomaly and a marked negative Eu anomaly (Fig. 6d). It would appear that the protolith of the felsic gneiss was

Please cite this article as: Xu, W.-C., et al., Rapid Eocene erosion, sedimentation and burial in the eastern Himalayan syntaxis and its geodynamic significance, Gondwana Res. (2012), doi:10.1016/j.gr.2012.05.011

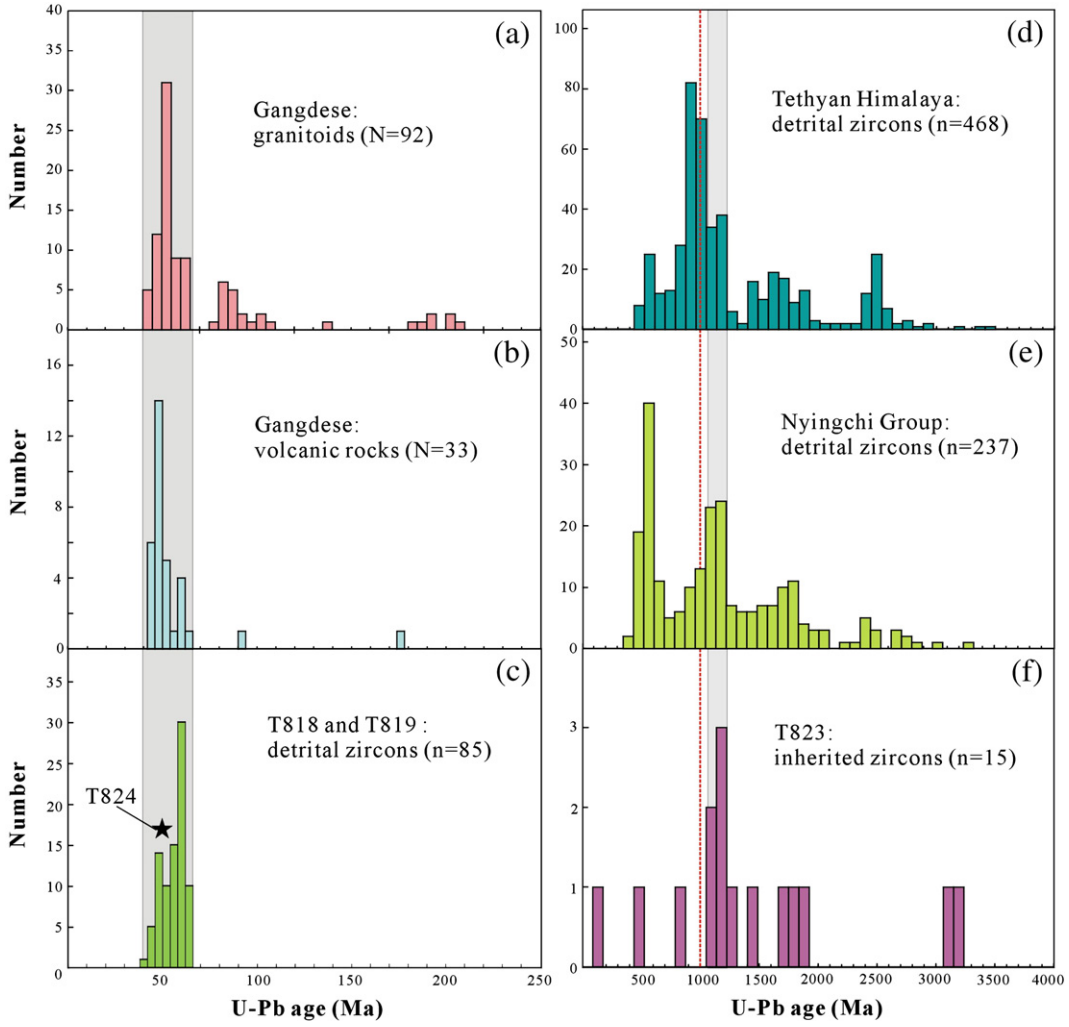

Fig. 7. U–Pb zircon age histograms. (a) Gangdese granitoids; (b) Gangdese volcanic rocks; (c) metasedimentary rocks from the lower Bomi Group; (d) Tethyan sedimentary rocks; (e) metasedimentary rocks for the lower Nyingchi Group; and (f) leucosome sample T823 in the lower Bomi Group. N = number of samples, n = total number of analyses. Star indicates age of the felsic gneiss sample T824. The $^{207}Pb/^{206}Pb$ ages were used for those older than 1000 Ma, and $^{206}Pb/^{238}U$ ages were used for younger zircons.
Data sources are from Coulon et al. (1986), Zhou et al. (2004), Dong et al. (2005), Mo et al. (2005), McQurrie et al. (2008), Wen et al. (2008), Zhang et al. (2008), Ji et al. (2009), Lee et al. (2009), Myrow et al. (2009, 2010), Dong et al. (2010) and Zhu et al. (2008, 2011a, b).

~50.6 Ma old and it was metamorphosed to create rims during ~38–27 Ma.

5. Discussion

5.1. Provenance and tectonic affinity of the lower Bomi Group

The lower Bom\i Group of Lhasa terrane consists of gneiss, mica schist, migmatite, amphibolite and marble, all of which have been metamorphosed under upper-amphibolite facies conditions. Previous studies have revealed that the protoliths of the mica schists are pyroclastics (XBGMR, 1995; Zheng et al., 2003). This is consistent with their petrography and zircon morphology. Both mica schist and marble are supracrustal components of the lower Bomi Group. Most of the analyzed cores of zircon grains from the mica schist (sample T818) and the marble (sample T819) preserve an oscillatory zoning pattern and have relatively high Th/U values of >0.2, indicating that these inherited detrital zircons are of magmatic origin (Corfu et al., 2003). Furthermore, these zircon cores have relatively high REE contents and distinctly fractionated REE patterns, with enrichment in HREE and depletion of LREE, typical of magmatic zircons (Hoskin and Schaltegger, 2003). Thus, their U–Pb zircon ages would indicate the magmatic events of the provenance of the lower Bomi Group. The detrital zircon ages from the marble (sample T819) and the mica schist (sample T818) range from ~62 Ma to ~41.5 Ma and between ~63 Ma and ~46.8 Ma, respectively; no ages older than 63 Ma have been found. These ages from the detrital zircons are consistent with the magma crystallization ages of the Gangdese magmatic arc (Fig. 7a, b), suggesting that the Gangdese magmatic arc could be the provenance for the lower Bomi Group. The Gangdese magmatic arc, the southernmost part of the Asian continent, is characterized by extensive Jurassic–Paleogene calc-alkaline granitoids (Wen et al., 2008; Ji et al., 2009; Chu et al., 2011; Zhu et al., 2011b) and Cretaceous to Paleogene non-marine volcanic sequences (e.g. the Linzizong Formation) (Mo et al., 2003; Zhou et al., 2004; Mo et al., 2008; Lee et al., 2009). Geochronological data show that the ~65–41 Ma is the most prominent period of magmatism in the Lhasa terrane (Fig. 7a, b). The abundant Paleogene ages and the absence of older ages (>63 Ma) of the detrital zircons indicate that the Gangdese magmatic arc could be the only source for the lower Bomi Group. The rapid uplift since ~40 Ma ago and subsequent erosion of the east Gangdese arc (Chung et al., 1998) is consistent with the sedimentation records from the lower Bomi Group.

The minimum detrital magmatic zircon age (~41.5 Ma) from the marble implies that the maximum depositional age for the lower Bomi Group is less than ~41.5 Ma. Thus we conclude that the lower Bomi Group cannot represent Precambrian basement for

the Lhasa terrane as has been previously assumed (Li, 1955; Dewey et al., 1988; Zheng et al., 2003). This is consistent with the findings of some recent studies on the Nyingchi Group in the western margin of the EHS and the Nyainqentanglha Group in the central Lhasa terrane (Zhang et al., 2008; Dong et al., 2010, 2011). We suggest that the lower Bomi Group may represent sediments from the residual forearc basin, similar to the Tsojiangding Group in the Xigaze area. The Tsojiangding Group unconformably overlies the Xigaze Group, and deposited during Paleocene (Dürr, 1996; Ding et al., 2005; Jia et al., 2005; Wu et al., 2010). It is composed of conglomerate, foraminifera-bearing sandy limestone and sandstone (Ding et al., 2005). However, the absence of ages of detrital zircons for the Tsojiangding Group has precluded further comparing with the lower Bomi Group.

In this study, the mantles of zircon grains from the felsic gneiss (sample T824) show oscillatory zoning, high Th/U ratios and REE contents and distinctly fractionated REE patterns, with enrichment in HREE and depletion of LREE, which are typical for magmatic zircon (Corfu et al., 2003; Hoskin and Schaltegger, 2003). The mantles yielded a weighted mean $^{206}Pb/^{238}U$ age of 50.6 ± 0.8 Ma (2σ; MSWD = 0.4). As discussed above, the Gangdese magmatic arc is characterized by ~65–41 Ma magmatism. Thus, the felsic gneisses would correlate to the Gangdese granitoids in southern Lhasa terrane in provenance.

Importantly, the inherited zircon cores from the leucosome (sample T823) yield a wide U–Pb age range from ~171 Ma to ~3211 Ma, with a prominent cluster at 1200–1050 Ma (Fig. 7f). The age population of the leucosome is different from its corresponding mesosome (sample T824), suggesting that the leucosome was not derived from the partial melting of the mesosome. Recently, Zhu et al. (2011a) published a set of U–Pb age data on detrital zircons from Paleozoic metasedimentary rocks in the Lhasa terrane. These U–Pb ages define a distinctive age population of ~1170 Ma, whereas those from the Tethyan Himalaya terrane define an age population of ~950 Ma (Fig. 7d). In the EHS, the detrital zircons from the lower Nyingchi Group also define an age population of ~1170 Ma (Fig. 7e), similar to the Paleozoic metasedimentary rocks in the Lhasa terrane. For the leucosome, the distinctive ~1180 Ma age population of inherited zircons matches well with that of detrital zircons in the lower Nyingchi Group (Fig. 7e, f). This correlation suggests that the leucosome in the lower Bomi Group was likely derived from partial melting of the lower Nyingchi Group or its equivalent. Therefore, we propose that the sediments in the lower Bomi Group have deposited on the lower Nyingchi Group or its equivalent prior to the Indian plate subduction. During the following subduction, partial melting of the lower Nyingchi Group or its equivalent produced leucocratic magma, which intruded the overlying sediments and the Gangdese granitoids.

5.2. Eocene metamorphism of lower Bomi Group

The Tibetan–Himalayan orogen was largely created by the India–Asian collision at ~55 Ma as suggested by multidisciplinary lines of both direct and indirect evidence (Allègre et al., 1984; Patriat and Achache, 1984; Rowley, 1996; Zhu et al., 2005; Chen et al., 2010; Najman et al., 2010; Sun et al., 2010, 2012; Cai et al., 2011; Clementz et al., 2011; Wang et al., 2011). Exposures of HP metamorphic rocks within the Himalayan orogen provide crucial insights into the collision, continental subduction and exhumation process (Tonarini et al., 1993; Guillot et al., 1997; Ding et al., 2001). In the western Himalaya, the coesite-bearing UHP eclogites, occurring in the Tso Morari and Kaghan areas, have demonstrated that the continental crust of the entire northwestern part of the Indian plate was subducted beneath the Kohistan–Ladakh arc to a minimum depth of 90 km (O'Brien et al., 2001; Mukherjee et al., 2003). Geochronological investigations for the UHP eclogites show that their peak-pressure metamorphism occurred in the Early Eocene (55–46 Ma) and then exhumed rapidly to upper crust depth before ~40 Ma (de Sigoyer et al., 2000; Kaneko et al., 2003; Leech et al., 2005; Parrish et al., 2006). It implies a rapid geodynamic process of continental subduction followed by exhumation in the western Himalaya.

In the EHS, HP granulites are present in the Himalayan unit but as yet no eclogite has been identified (Zhong and Ding, 1996; Liu and Zhong, 1997). Geochronological study of the granulite-facies metamorphic rocks has yielded contentious results, with peak metamorphic age ranging from ~40 Ma to ~24 Ma (Ding et al., 2001; Liu et al., 2007b; Xu et al., 2010; Zhang et al., 2010b; Su et al., 2012). As a result, the subduction process in the eastern part of the orogen is poorly constrained. Recently, Zhang et al. (2010b) proposed that the eastern Himalayan syntaxis represents a paired metamorphic belt formed during the Cenozoic Himalayan collisional orogeny. The hanging wall (the southern Lhasa terrane) is characterized by the high-temperature conditions with abundant granite intrusion, while the footwall (the Himalayan unit) registers penecontemporaneous HP metamorphism. We now propose that some lithologies within the hanging wall could also be involved in the subduction process.

The lower Bomi Group, which now lies in the hanging wall of the continental subduction zone in the Lhasa terrane, has been subjected to amphibolite-facies metamorphism. The zircons from the mica schist, marble and felsic gneiss examined in this study generally show metamorphic rims characterized by uniform CL images and lacking any zoning. Moreover, these zircon rims show equal or lower REE contents than their inherited magmatic zircon precursors, and some have very low Th/U values (0.01–0.02), typical of metamorphic zircons (Hoskin and Schaltegger, 2003; Harley and Kelly, 2007). Our geochronological work indicates that amphibolite-grade metamorphism was initiated at ~38 Ma and continued to ~24 Ma, as recorded in zircon rims from both the metamorphic supracrustal rocks and the felsic gneiss. Furthermore, the age of 36.9 ± 0.5 Ma from zircons taken from the leucosome of the migmatite provides a precise age for crustal melting. The ~37 Ma zircon rims from leucosome T823 are HREE depleted and show flat HREE patterns, similar to values expected for HP metamorphic zircons that grew in competition with garnet (Fig. 6c) (Rubatto, 2002; Rubatto and Hermann, 2007). The initial time of metamorphism is thus in good agreement with the time of the anatexis and also with metamorphic ages recorded in the Nyingchi Group in the EHS (Zhang et al., 2010b). In order to explain the medium-grade metamorphism in the supracrustal rocks, we propose that following the Indian–Asian collision, the forearc sediments were subducted into the middle-lower crust, together with Himalayan lithologies from the Indian continental slab. The metamorphism in the hanging wall, therefore, indicates that the India–Asia collision and the following subduction of the Indian plate beneath Asia were initiated at least before ~37 Ma in the EHS. In the Namche Barwa Group of the Himalayan unit, similar metamorphic ages of ~37–32 Ma associated with the Indian continental subduction were reported by Zhang et al. (2010b). The protracted time of the Indian continental subduction recorded in both the hanging wall and footwall of the subduction zone in the EHS is markedly later than that in the western Himalaya, where the deep subduction rocks had exhumed to the upper crust depth before ~40 Ma (de Sigoyer et al., 2000; Leech et al., 2005; Parrish et al., 2006). This observation might reflect real diachroneity in the timing of subduction of the Indian continent along the length of the Himalayan orogen (Guillot et al., 2008; Zhang et al., 2010b), although the metamorphic history of the eastern and western parts of the Himalayan belt appear to become broadly synchronous after ~24 Ma (Xu et al., 2010; Su et al., 2012).

5.3. Tectonic implication and a model for the EHS in the Paleogene

Our results demonstrate that the lithologies of the lower Bomi Group have been subducted to a sufficient depth to produce the amphibolite-facies metamorphism as early as the ~37 Ma. Since the

Please cite this article as: Xu, W.-C., et al., Rapid Eocene erosion, sedimentation and burial in the eastern Himalayan syntaxis and its geodynamic significance, Gondwana Res. (2012), doi:10.1016/j.gr.2012.05.011

minimum age of detrital magmatic zircons from the supracrustal rocks is ~41.5 Ma, it implies that the magmatism, crustal uplift and erosion of provenence, sedimentation and metamorphism for the lower Bomi Group had taken place in a short time interval (<5 Ma), suggesting a rapid geodynamic process during the Late Eocene in the EHS. The rapid process had also happened at Late Paleocene–Early Eocene in the western Himalaya. Leech et al. (2005) attributed the rapid process to the initial India–Asian collision and the subsequent subduction of the leading edge of India continental plate at a steep angle. This interpretation is also suitable for the EHS.

Our data do not support a tectonic model in which the forearc basin was underthrust along the north-dipping Gangdese thrust during the Oligo-Miocene (Yin et al., 1994, 1999) but instead indicate that it was the continental subduction of the Indian plate that entrained the southern edge of the Lhasa terrane (the forearc sediment) into the middle-lower crust during Late Eocene. Considering the petrological and geochronological studies presented above, we propose a model of forearc sedimentation followed by imbrication and subduction of the basin to explain the evolution of the lower Bomi Group of the southern margin of the Lhasa terrane (Fig. 8). Rollback and breakoff of the Neotethyan oceanic slab at ~60–50 Ma in the eastern Himalayan orogen (Chung et al., 2005; Lee et al., 2009), resulted in a marked intensification of magmatism in the Lhasa terrane, as indicated by large volumes of Linzizong volcanic rocks and the intrusion of Gangdese Batholith at ~65–41 Ma (Lee et al., 2009). The persistent northward drift of India resulted in thickening of the Tibetan continental lithosphere, isostatic uplift and erosion of the Lhasa terrane. The denuded materials were deposited into the forearc basin to the south. Continuing subduction of the Indian continent beneath Asia caused the basin lithologies to be involved in imbrication and subduction, resulting in the observed amphibolite-facies metamorphism. Simultaneously, anatectic melt derived from the basement of the Lhasa terrane was injected into the lower Bomi Group.

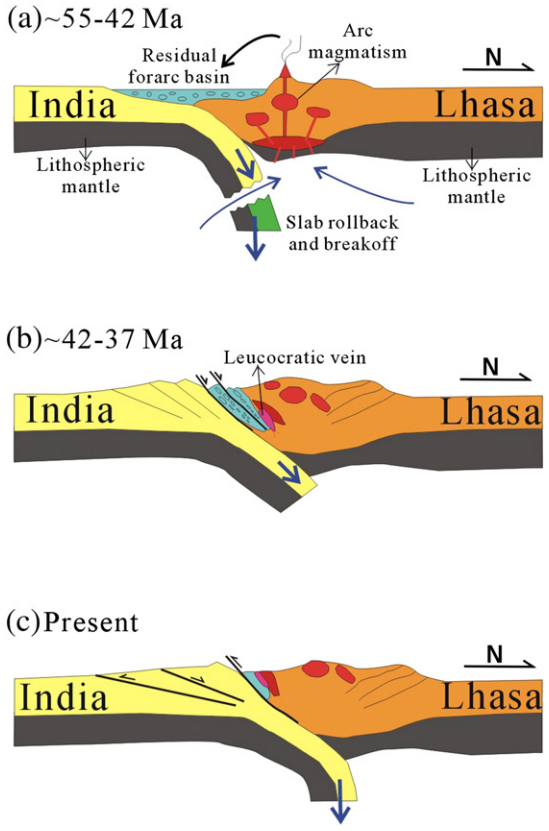

Fig. 8. Proposed geodynamic model of the eastern Himalayan syntaxis inferred from the analytical results obtained in this study. a. After the Indian–Asian collision at ~55 Ma, the lower Bomi Group may have been deposited in a residual forearc basin that developed on the southern side of the Gangdese magmatic arc. b. During ~42–37 Ma, the basin sediment had been involved into the subduction zone by imbricate slicing, and been subducted to deeper levels, resulting in the observed amphibolite-facies metamorphism. c. The previously subducted metasedimentary rocks and the granitic gneisses have exhumed to the surface at present.

6. Conclusions

Petrographic and geochronological studies show that the lower Bomi Group in the east Himalayan syntaxis formed later than ~42 Ma and was dominantly sourced from the Gangdese magmatic arc. The lithologies of the lower Bomi Group are inferred to represent a forearc basin. The lower Bomi Group was subducted during the Late Eocene and subjected to amphibolite-facies metamorphism at ~37 Ma. During the Late Eocene in the EHS, a series of events, including the erosion of the Gangdese arc, sedimentation, burial and metamorphism, had taken place within a short time interval (<5 Ma). This suggests a rapid geodynamic process that associated with the initial India–Asian collision and the following subduction of the leading edge of India continental plate at a steep angle during the Eocene in the EHS. The protracted time of the Indian continental subduction in the eastern Himalaya is markedly later than that in the western Himalaya, suggesting diachroneity in the timing of subduction of the Indian continent along the strike of the Himalayan orogen.

Acknowledgments

This research is supported by the Natural Science Foundation of China (grants: 41073046 and 41103019), the National Key Project for Basic Research (no. 2011CB403102), China Geological Survey (no. 1212011121261), SinoProb 04-02, the Fundamental Research Funds for National University and the Foundation for Open Projects of State Key Laboratory of Geological Processes and Mineral Resources, China University of Geosciences (GPMR201009).

Appendix A. Supplementary data

Supplementary data to this article can be found online at http://dx.doi.org/10.1016/j.gr.2012.05.011.

References

Allègre, C., Courtillot, V., Tapponnier, P., Hirn, A., Mattauer, M., Coulon, C., Jaeger, J., Achache, J., Schaerer, U., Marcoux, J., 1984. Structure and evolution of the Himalaya–Tibet orogenic belt. Nature 307, 17–22.

Andersen, T., 2002. Correction of common lead in U–Pb analyses that do not report ^{204}Pb. Chemical Geology 192, 59–79.

Booth, A.L., Zeitler, P.K., Kidd, W.S.F., Wooden, J., Liu, Y.P., B., I., Hern, M., Chamberlain, C.P., 2004. U–Pb zircon constraints on the tectonic evolution of southeastern Tibet, Namche Barwa area. American Journal of Science 304, 889–929.

Booth, A.L., Chamberlain, C.P., Kidd, W.S.F., Zeitler, P.K., 2009. Constraints on the metamorphic evolution of the eastern Himalayan syntaxis from geochronologic and petrologic studies of Namche Barwa. Geological Society of America Bulletin 121, 385–407.

Boyton, W., 1984. Geochemistry of the rare earth elements: meteorite studies. In: Henderson, P. (Ed.), Rare Earth Element Geochemistry, pp. 63–114.

Bozhilov, K., Green, H., Dobrzhinetskaya, L., 1999. Clinoenstatite in Alpe Arami peridotite: additional evidence of very high pressure. Science 284, 128–132.

Burg, J., Davy, P., Nievergelt, P., Oberli, F., Seward, D., Diao, Z., Meier, M., 1997. Exhumation during crustal folding in the Namche-Barwa syntaxis. Terra Nova 9, 53–56.

Burg, J.-P., Nievergelt, P., Oberli, F., Seward, D., Davy, P., Maurin, J.-C., Diao, Z., Meier, M., 1998. The Namche Barwa syntaxis: evidence for exhumation related to compressional crustal folding. Journal of Asian Earth Sciences 16, 239–252.

Cai, F.L., Ding, L., Yue, Y.H., 2011. Provenance analysis of upper Cretaceous strata in the Tethys Himalaya, southern Tibet: implications for timing of India–Asia collision. Earth and Planetary Science Letters 305, 195–206.

Chen, J., Huang, B., Sun, L., 2010. New constraints to the onset of the India–Asia collision: paleomagnetic reconnaissance on the Linzizong Group in the Lhasa Block, China. Tectonophysics 489, 189–209.

Chiu, H.Y., Chung, S.L., Wu, F.Y., Liu, D.Y., Liang, Y.H., Lin, I.-J., Iizuka, Y., Xie, L.W., Wang, Y.B., Chu, M.F., 2009. Zircon U–Pb and Hf isotopic constraints from eastern

Transhimalayan batholiths on the precollisional magmatic and tectonic evolution in southern Tibet. Tectonophysics 477, 3–19.
Chu, M.F., Chung, S.L., Song, B.A., Liu, D.Y., O'Reilly, S.Y., Pearson, N.J., Ji, J.Q., Wen, D.J., 2006. Zircon U–Pb and Hf isotope constraints on the Mesozoic tectonics and crustal evolution of southern Tibet. Geology 34, 745–748.
Chu, M.F., Chung, S.L., O'Reilly, S.Y., Pearson, N.J., Wu, F.Y., Li, X.H., Liu, D.Y., Ji, J.Q., Chu, C.H., Lee, H.Y., 2011. India's hidden inputs to Tibetan orogeny revealed by Hf isotopes of Transhimalayan zircons and host rocks. Earth and Planetary Science Letters 307, 479–486.
Chung, S.L., Lo, C.H., Lee, T.Y., Zhang, Y.Q., Xie, Y.W., Li, X.H., Wang, K.L., Wang, P.L., 1998. Diachronous uplift of the Tibetan Plateau starting 40 Myr ago. Nature 394, 769–773.
Chung, S.L., Liu, D.Y., Ji, J.Q., Chu, M.F., Lee, H.Y., Wen, D.J., Lo, C.H., Lee, T.Y., Qian, Q., Zhang, Q., 2003. Adakites from continental collision zones: melting of thickened lower crust beneath southern Tibet. Geology 31, 1021–1024.
Chung, S.L., Chu, M.F., Zhang, Y.Q., Xie, Y.W., Lo, C.H., Lee, T.Y., Lan, C.Y., Li, X.H., Zhang, Q., Wang, Y.Z., 2005. Tibetan tectonic evolution inferred from spatial and temporal variations in post-collisional magmatism. Earth-Science Reviews 68, 173–196.
Clementz, M., Bajpai, S., Ravikant, V., Thewissen, J.G.M., Saravanan, N., Singh, I.B., Prasad, V., 2011. Early Eocene warming events and the timing of terrestrial faunal exchange between India and Asia. Geology 39, 15–18.
Corfu, F., Hanchar, J., Hoskin, P., Kinny, P., 2003. Atlas of zircon textures. Reviews in Mineralogy and Geochemistry 53, 469–500.
Cottle, J., Searle, M., Horstwood, M., Waters, D., 2009. Timing of midcrustal metamorphism, melting, and deformation in the Mount Everest region of southern Tibet revealed by U (–Th)–Pb geochronology. The Journal of Geology 117, 643–664.
Coulon, C., Maluski, H., Bollinger, C., Wang, S., 1986. Mesozoic and Cenozoic volcanic rocks from central and southern Tibet: ^{39}Ar–^{40}Ar dating, petrological characteristics and geodynamical significance. Earth and Planetary Science letters 79, 281–302.
Dürr, S., 1996. Provenance of Xigaze fore-arc basin clastic rocks (Cretaceous, south Tibet). Bulletin of the Geological Society of America 108, 669–684.
de Sigoyer, J., Chavagnac, V., Blichert-Toft, J., Villa, I.M., Luais, B., Guillot, S., Cosca, M., Mascle, G., 2000. Dating the Indian continental subduction and collisional thickening in the northwest Himalaya: multichronology of the Tso Morari eclogites. Geology 28, 487–490.
Dewey, J., Shackleton, R., Chengfa, C., Yiyin, S., 1988. The tectonic evolution of the Tibetan Plateau. Philosophical Transactions of the Royal Society of London. Series A, Mathematical and Physical Sciences 379–413.
Ding, L., Zhong, D., 1999. Metamorphic characteristics and geotectonic implications of the high-pressure granulites from Namjagbarwa, eastern Tibet. Science in China (Earth sciences) 42, 491–505.
Ding, L., Zhong, D.L., Yin, A., Kapp, P., Harrison, T.M., 2001. Cenozoic structural and metamorphic evolution of the eastern Himalayan syntaxis (Namche Barwa). Earth and Planetary Science Letters 192, 423–438.
Ding, L., Kapp, P., Wan, X., 2005. Paleocene–Eocene record of ophiolite obduction and initial India–Asia collision, south central Tibet. Tectonics 24 (TC3001) doi: 3010.1029/2004TC001729.
Dobrzhinetskaya, L., Green, H.W., Wang, S., 1996. Alpe Arami: a peridotite massif from depths of more than 300 kilometers. Science 271, 1841–1845.
Dong, G.C., Mo, X.X., Zhao, Z.D., Guo, T.Y., Wang, L.L., Chen, T., 2005. Geochronologic constraints on the magmatic underplating of the Gangdise belt in the India–Eurasia collision: evidence of SHRIMP II zircon U–Pb dating. Acta Geologica Sinica 79, 787–794.
Dong, X., Zhang, Z.M., Santosh, M., 2010. Zircon U–Pb chronology of the Nyingtri Group, southern Lhasa terrane, Tibetan Plateau: implications for Grenvillian and Pan-African provenance and Mesozoic–Cenozoic metamorphism. The Journal of Geology 118, 677–690.
Dong, X., Zhang, Z., Liu, F., Wang, W., Yu, F., Shen, K., 2011. Zircon U–Pb geochronology of the Nyainqentanglha Group from the Lhasa terrane: new constraints on the Triassic orogeny of the south Tibet. Journal of Asian Earth Sciences 42, 732–739.
Geng, Q.R., Pan, G.T., Zheng, L.L., Sun, Z.M., Qu, C.S., Dong, H., 2004. Petrological characteristics and original settings of the Yarlung Tsangpo ophiolitic mélange, Namche Barwa, SE Tibet. Chinese Journal of Geology 39, 1–19 (in Chinese with English abstract).
Geng, Q.R., Pan, G.T., Zheng, L.L., Chen, Z.L., Fisher, R.D., Sun, Z.M., Ou, C.S., Dong, H., Wang, X.W., Li, S., Lou, X.Y., Fu, H., 2006. The eastern Himalayan syntaxis: major tectonic domains, ophiolitic mélanges and geologic evolution. Journal of Asian Earth Sciences 27, 265–285.
Guan, Q., Zhu, D.C., Zhao, Z.D., Dong, G.C., Zhang, L.L., Li, X.W., Liu, M., Mo, X.X., Liu, Y.S., Yuan, H.L., 2012. Crustal thickening prior to 38 Ma in southern Tibet: evidence from lower crust-derived adakitic magmatism in the Gangdese Batholith. Gondwana Research 21, 88–99.
Guillot, S., de Sigoyer, J., Lardeaux, J., Mascle, G., 1997. Eclogitic metasediments from the Tso Morari area (Ladakh, Himalaya): evidence for continental subduction during India–Asia convergence. Contributions to Mineralogy and Petrology 128, 197–212.
Guillot, S., Mahéo, G., de Sigoyer, J., Hattori, K.H., Pêcher, A., 2008. Tethyan and Indian subduction viewed from the Himalayan high- to ultrahigh-pressure metamorphic rocks. Tectonophysics 451, 225–241.
Guo, L., Zhang, H.F., Xu, W.C., 2008. U–Pb zircon ages of migmatite and granitic gneiss from Duoxiongla in eastern Himalayan syntaxis and their geological implications. Acta Petrologica Sinica 24, 421–429 (in Chinese with English abstract).
Guo, L., Zhang, H.F., Harris, N., Pan, F.B., Xu, W.C., 2011. Origin and evolution of multistage felsic melts in eastern Gangdese belt: constraints from U–Pb zircon dating and Hf isotopic composition. Lithos 127, 54–67.
Guo, L., Zhang, H.F., Harris, N., Parrish, R., Xu, W.C., Shi, Z.L., 2012. Paleogene crustal anatexis and metamorphism in Lhasa terrane, eastern Himalayan syntaxis: evidence from U–Pb zircon and Hf isotopic compositions of the Nyingchi Complex. Gondwana Research 21, 100–111.
Harley, S., Kelly, N., 2007. Zircon tiny but timely. Elements 3, 13–18.
Harris, N.B.W., Holland, T.J.B., Tindle, A.G., 1988. Metamorphic rocks of the 1985 Tibet geotraverse, Lhasa to Golmud. Philosophical Transactions of the Royal Society of London, Series A 327, 203–213.
Hoskin, P., Schaltegger, U., 2003. The composition of zircon and igneous and metamorphic petrogenesis. Reviews in Mineralogy and Geochemistry 53, 27–62.
Hu, Z.C., Gao, S., Liu, Y.S., Hu, S.H., Chen, H.H., Yuan, H.L., 2008. Signal enhancement in laser ablation ICP–MS by addition of nitrogen in the central channel gas. Journal of Analytical Atomic Spectrometry 23, 1093–1101.
Ji, W.Q., Wu, F.Y., Chung, S.L., Li, J.X., Liu, C.Z., 2009. Zircon U–Pb geochronology and Hf isotopic constraints on petrogenesis of the Gangdese Batholith, southern Tibet. Chemical Geology 262, 229–245.
Jia, J.C., Wen, C.S.W., G.H., Zhang, Z.L., Wang, L.J., 2005. New understanding of stratum of Xigaze forearc basin in the north of Qiongguo area, Zhongba, Tibet. North Western Geology 35, 33–39 (in Chinese with English abstract).
Kaneko, Y., Katayama, I., Yamamoto, H., Misawa, K., Ishikawa, M., Rehman, H., Kausar, A., Shiraishi, K., 2003. Timing of Himalayan ultrahigh-pressure metamorphism: sinking rate and subduction angle of the Indian continental crust beneath Asia. Journal of Metamorphic Geology 21, 589–599.
Lee, H.Y., Chung, S.L., Lo, C.H., JI, J.Q., Lee, T.Y., Qian, Q., Zhang, Q., 2009. Eocene Neotethyan slab breakoff in southern Tibet inferred from the Linzizong volcanic record. Tectonophysics 477, 20–35.
Leech, M.L., Singh, S., Jain, A.K., Klemperer, S.L., Manickavasagam, R.M., 2005. The onset of India–Asia continental collision: early, steep subduction required by the timing of UHP metamorphism in the western Himalaya. Earth and Planetary Science Letters 234, 83–97.
Li, P., 1955. Primary understanding of geology, eastern Tibet. Chinese Science Bulletin 7, 62–71.
Li, Z.L., Yang, J.S., Xu, Z.Q., Li, T.F., Xu, X.Z., Ren, Y.F., Robinson, P.T., 2009. Geochemistry and Sm–Nd and Rb–Sr isotopic composition of eclogite in the Lhasa terrane, Tibet, and its geological significance. Lithos 109, 240–247.
Liu, Y., Zhong, D., 1997. Petrology of high-pressure granulites from the eastern Himalayan syntaxis. Journal of Metamorphic Geology 15, 451–466.
Liu, L., Zhang, J., Green, I., Harry, W., Jin, Z., Bozhilov, K.N., 2007a. Evidence of former stishovite in metamorphosed sediments, implying subduction to >350 km. Earth and Planetary Science Letters 263, 180–191.
Liu, Y., Yanc, Z.Q., Wang, M., 2007b. History of zircon growth in a high-pressure granulite within the eastern Himalayan syntaxis, and tectonic implications. International Geology Review 49, 861–872.
Liu, F., Gerdes, A., Zeng, L., Xue, H., 2008a. SHRIMP U–Pb dating, trace elements and the Lu–Hf isotope system of coesite-bearing zircon from amphibolite in the SW Sulu UHP terrane, eastern China. Geochimica Et Cosmochimica Acta 72, 2973–3000.
Liu, Y.S., Hu, Z.C., Gao, S., Günther, D., Xu, J., Gao, C.G., Chen, H.H., 2008b. In situ analysis of major and trace elements of anhydrous minerals by LA-ICP-MS without applying an internal standard. Chemical Geology 257, 34–43.
Liu, Y.S., Gao, S., Hu, Z.C., Gao, C.G., Zong, K.Q., Wang, D.B., 2010a. Continental and oceanic crust recycling-induced melt–peridotite interactions in the Trans-North China Orogen: U–Pb dating, Hf isotopes and trace elements in zircons of mantle xenoliths. Journal of Petrology 51, 537–571.
Liu, Y.S., Hu, Z.C., Zong, K.Q., Gao, C.G., Gao, S., Xu, J., Chen, H., 2010b. Reappraisement and refinement of zircon U–Pb isotope and trace element analyses by LA-ICP-MS. Chinese Science Bulletin 55, 1535–1546.
Ludwig, K.R., 2003. ISOPLOT 3.0: A Geochronological Toolkit for Microsoft Excel. Berkeley Geochronology Center, Berkeley, California.
McQurrie, N., Robinson, D., Long, S., Tobgay, T., Grujic, D., Gehrels, G., Duce, M., 2008. Preliminary stratigraphic and structural architecture of Bhutan: implications for the along strike architecture of the Himalayan system. Earth and Planetary Science letters 272, 105–117.
Mo, X., Zhao, Z., Deng, J., Dong, G., Zhou, S., Guo, T., Zhang, S., Wang, L., 2003. Response of volcanism to the India–Asia collision. Earth Science Frontiers 10, 135–148 (in Chinese with English abstract).
Mo, X.X., Dong, G.C., Zhao, Z.D., Guo, T.Y., Wang, L.L., Chen, T., 2005. Timing of magma mixing in the Gangdise magmatic belt during the India–Asia collision: zircon SHRIMP U–Pb dating. Acta Geologica Sinica 79, 66–76.
Mo, X.X., Hou, Z., Niu, Y., Dong, G., Qu, X., Zhao, Z., Yang, Z., 2007. Mantle contributions to crustal thickening during continental collision: evidence from Cenozoic igneous rocks in southern Tibet. Lithos 96, 225–242.
Mo, X.X., Niu, Y.L., Dong, G.C., Zhao, Z.D., Hou, Z.Q., Su, Z., Ke, S., 2008. Contribution of syncollisional felsic magmatism to continental crust growth: a case study of the Paleogene Linzizong volcanic succession in southern Tibet. Chemical Geology 250, 49–67.
Myrow, P.M., Hughes, N.C., Searle, M.P., Panning, C.M., Peng, S.C., Parcha, S.K., 2009. Stratigraphic correlation of Cambrian–Ordovician deposits along the Himalaya: implications for the age and nature of rocks in the Mount Everest region. Bulletin of the Geological Society of America 120, 323–332.
Myrow, P.M., Hughes, N.C., Goodge, J.W., Fanning, C.M., Williams, I.S., Peng, S.C., Bhargava, O.N., Parcha, S.K., Pogue, K.R., 2010. Extraordinary transport and mixing of sediment across Himalayan central Gondwana during the Cambrian–Ordovician. Bulletin of the Geological Society of America 122, 1660–1670.
Mukherjee, B., Sachan, H., Ogasawara, Y., Muko, A., Yoshioka, N., 2003. Carbonate-bearing UHPM rocks from the Tso-Morari region, Ladakh, India: petrological implications. International Geology Review 45, 49–69.

Please cite this article as: Xu, W.-C., et al., Rapid Eocene erosion, sedimentation and burial in the eastern Himalayan syntaxis and its geodynamic significance, Gondwana Res. (2012), doi:10.1016/j.gr.2012.05.011

Najman, Y., Appel, E., Boudagher-Fadel, M., Bown, P., Carter, A., Garzanti, E., Godin, L., Han, J., Liebke, U., Oliver, G., Parrish, R., Vezzoli, G., 2010. Timing of India–Asia collision: geological, biostratigraphic, and palaeomagnetic constraints. Journal of Geophysical Research 115, B12416.
O'Brien, P., Zotov, N., Law, R., Khan, M., Jan, M., 2001. Coesite in Himalayan eclogite and implications for models of India–Asia collision. Geology 29, 435–438.
Patriat, P., Achache, J., 1984. India–Eurasia collision chronology has implications for crustal shortening and driving mechanism of plates. Nature 311, 615–621.
Parrish, R., Gough, S., Searle, M., Waters, D., 2006. Plate velocity exhumation of ultrahigh-pressure eclogites in the Pakistan Himalaya. Geology 34, 989–992.
Rowley, D., 1996. Age of initiation of collision between India and Asia: a review of stratigraphic data. Earth and Planetary Science Letters 145, 1–13.
Rubatto, D., 2002. Zircon trace element geochemistry: partitioning with garnet and the link between U–Pb ages and metamorphism. Chemical Geology 184, 123–138.
Rubatto, D., Hermann, J., 2007. Zircon behaviour in deeply subducted rocks. Elements 3, 31–35.
Su, W., Zhang, M., Liu, X., Lin, J., Ye, K., 2012. Exact timing of granulite metamorphism in the Namche-Barwa, eastern Himalayan syntaxis: new constrains from SIMS U–Pb zircon age. International Journal of Earth Sciences 101, 239–252.
Sun, Z.M., Jiang, W., Li, H., Pei, J., Zhu, Z., 2010. New paleomagnetic results of Paleocene volcanic rocks from the Lhasa block: tectonic implications for the collision of India and Asia. Tectonophysics 490, 257–266.
Sun, Z.M., Pei, J.L., Li, H.B., Xu, W., Jiang, W., Zhu, Z.M., Wang, X.S., Yang, Z.Y., 2012. Palaeomagnetism of late Cretaceous sediments from southern Tibet: evidence for the consistent palaeolatitudes of the southern margin of Eurasia prior to the collision with India. Gondwana Research 21, 53–63.
Tonarini, S., Villa, I., Oberli, F., Meier, M., Spencer, D., Pognante, U., Ramsay, J., 1993. Eocene age of eclogite metamorphism in Pakistan Himalaya: implications for India-Eurasia collision. Terra Nova 5, 13–20.
Vavra, G., Gebauer, D., Schmid, R., Compston, W., 1996. Multiple zircon growth and recrystallization during polyphase Late Carboniferous to Triassic metamorphism in granulites of the Ivrea Zone (southern Alps): an ion microprobe (SHRIMP) study. Contributions to Mineralogy and Petrology 122, 337–358.
Vavra, G., Schmid, R., Gebauer, D., 1999. Internal morphology, habit and U–Th–Pb microanalysis of amphibolite-to-granulite facies zircons: geochronology of the Ivrea Zone (southern Alps). Contributions to Mineralogy and Petrology 134, 380–404.
Wang, J., Hu, X., Jansa, L., Huang, Z., 2011. Provenance of the upper Cretaceous–Eocene deep-water sandstones in Sangdanlin, southern Tibet: constraints on the timing of initial India–Asia collision. The Journal of Geology 119, 293–309.
Wen, D.R., Liu, D.Y., Chung, S.L., Chu, M.F., Ji, J.Q., Zhang, Q., Song, B., Lee, T.Y., Yeh, M.W., Lo, C.H., 2008. Zircon SHRIMP U–Pb ages of the Gangdese Batholith and implications for Neotethyan subduction in southern Tibet. Chemical Geology 252, 191–201.
Wiedenbeck, M., Wlle, P., Corfu, F., Griffin, W.L., Meier, M., Oberli, F., Quadt, A.V., Roddick, J.C., Spiegel, W., 1995. Three natural zircon standards for U–Th–Pb, Lu–Hf, trace element and REE analyses. Geostandards and Geoanalytical Research 19, 1–23.
Wu, F.Y., Ji, W.Q., Liu, C.Z., Chung, S.L., 2010. Detrital zircon U–Pb and Hf isotopic data from the Xigaze fore-arc basin: constraints on Transhimalayan magmatic evolution in southern Tibet. Chemical Geology 271, 13–25.
Wu, Y.B., Zheng, Y.F., 2004. Genesis of zircon and its constraints on interpretation of U–Pb age. Chinese Science Bulletin 49, 1554–1569.
XBGMR, 1995. The Regional Geology of Bomi and Tongmai (Geology Party) Scale 1:200,000 (in Chinese). Geological Publishing House, Beijing.
Xia, L.Q., Li, X.M., Ma, Z.P., Xu, X.Y., Xia, Z.C., 2011. Cenozoic volcanism and tectonic evolution of the Tibetan Plateau. Gondwana Research 19, 850–866.
Xu, S.T., Su, W., Liu, Y.C., Jiang, L.L., Ji, S.Y., Okay, A.I., Sengör, A.M.C., 1992. Diamond from the Dabie Shan metamorphic rocks and its implication for tectonic setting. Science 256, 80–82.
Xu, Z.Q., Cai, Z.H., Li, H.Q., Chen, F.Y., Tang, Z.M., 2008. Tectonics and fabric kinematics of the Namche Barwa terrane, eastern Himalayan syntaxis. Acta Geologica Sinica 24, 1463–1476 (in Chinese with English abstract).
Xu, W.C., Zhang, H.F., Parrish, R., Harris, N., Guo, L., Yuan, H.L., 2010. Timing of granulite-facies metamorphism in the eastern Himalayan syntaxis and its tectonic implications. Tectonophysics 485, 231–244.
Xu, Z.Q., Ji, S.C., Cai, Z.H., Zeng, L.S., Geng, Q.R., Cao, H., 2012. Kinematics and dynamics of the Namche Barwa syntaxis, eastern Himalaya: constraints from the deformation, fabrics and geochronology. Gondwana Research 21, 19–36.
Yang, J., Godard, G., Kienast, J.R., Lu, Y., Sun, J., 1993. Ultrahigh-pressure (60 kbar) magnesite-bearing garnet peridotites from northeastern Jiangsu, China. The Journal of Geology 101, 541–554.
Yang, J., Xu, Z., Li, Z., Xu, X., Li, T., Ren, Y., Li, H., Chen, S., Robinson, P.T., 2009. Discovery of an eclogite belt in the Lhasa block, Tibet: a new border for Paleo-Tethys? Journal of Asian Earth Sciences 34, 76–89.
Ye, K., Cong, B., Ye, D., 2000. The possible subduction of continental material to depths greater than 200 km. Nature 407, 734–736.
Yin, A., Harrison, T., Ryerson, F., Chen, W., Kidd, W., Copeland, P., 1994. Tertiary structural evolution of the Gangdese thrust system, southeastern Tibet. Journal of Geophysical Research 99, 18175–18201.
Yin, A., Harrison, T., Murphy, M., Grove, M., Nie, S., Ryerson, F., Xiaofeng, W., Zengle, C., 1999. Tertiary deformation history of southeastern and southwestern Tibet during the Indo–Asian collision. Bulletin of the Geological Society of America 111, 1644–1664.
Yin, A., Harrison, T.M., 2000. Geologic evolution of the Himalayan–Tibetan orogen. Annual Review of Earth and Planetary Sciences 28, 211–280.
Zeitler, P., Meltzer, A., Koons, P., Craw, D., Hallet, B., Chamberlain, C., Kidd, W., Park, S., Seeber, L., Bishop, M., 2001. Erosion, Himalayan geodynamics, and the geomorphology of metamorphism. GSA Today 11, 4–9.
Zhang, J.J., Ji, J.Q., Zhong, D.L., Ding, L., He, S.D., 2004. Structural pattern of eastern Himalayan syntaxis in Namjagbarwa and its formation process. Science in China (Earth sciences) 47, 138–150.
Zhang, H.F., Xu, W.C., Zong, K.Q., Yuan, H.L., Harris, N., 2008. Tectonic evolution of metasediments from the Gangdise terrane, Asian plate, eastern Himalayan syntaxis, Tibet. International Geology Review 50, 914–930.
Zhang, H.F., Harris, N., Guo, L.X., W.C., 2010a. The significance of Cenozoic magmatism from the western margin of the eastern syntaxis, southeast Tibet. Contributions to Mineralogy and Petrology 160, 83–98.
Zhang, Z.M., Zhao, G.C., Santosh, M., Wang, J.L., Dong, X., Liou, J.G., 2010b. Two stages of granulite facies metamorphism in the eastern Himalayan syntaxis, south Tibet: petrology, zircon geochronology and implications for the subduction of Neo-Tethys and the Indian continent beneath Asia. Journal of Metamorphic Geology 28, 719–733.
Zhang, Z.M., Zhao, G.C., Santosh, M., Wang, J.L., Dong, X., Shen, K., 2010c. Late Cretaceous charnockite with adakitic affinities from the Gangdese Batholith, southeastern Tibet: evidence for Neo-Tethyan mid-ocean ridge subduction? Gondwana Research 17, 615–631.
Zhang, Z.M., Dong, X., Santosh, M., Liu, F., Wang, W., Yiu, F., He, Z.Y., Shen, K., 2012. Petrology and geochronology of the Namche Barwa Complex in the eastern Himalayan syntaxis, Tibet: constraints on the origin and evolution of the north-eastern margin of the Indian Craton. Gondwana Research 21, 123–137.
Zheng, Y., 2003. Mineralogical evidence for continental deep subduction. Chinese Science Bulletin 48, 952–954.
Zheng, L.L., Dong, H., Geng, Q.R., Liao, G.Y., Sun, Z.M., Lou, X.Y., Li, S., 2003. 1:250,000 geological report of Motuo District with geological map. Chengdu Institute of Geology and Mineral Resources unpublished (in Chinese).
Zheng, Y.F., Ye, K., Zhang, L.F., 2009. Developing the plate tectonic from oceanic subduction to continental collision. Chinese Science Bulletin 54, 2549–2555.
Zhong, D.L., Ding, L., 1996. Discovery of high-pressure basic granulite in Namjagbarwa area, Tibet, China. Chinese Science Bulletin 41, 87–88.
Zhou, S., Mo, X.X., Dong, G.C., Zhao, Z.D., Qiu, R.Z., Guo, T.Y., Wang, L.L., 2004. ^{40}Ar–^{39}Ar geochronology of Cenozoic Linzizong volcanic rocks from Linzhou basin, Tibet, China, and their geological implications. Chinese Science Bulletin 49, 1970–1979.
Zhu, B., Kidd, W., Rowley, D., Currie, B., Shafique, N., 2005. Age of initiation of the India–Asia collision in the east-central Himalaya. The Journal of Geology 113, 265–285.
Zhu, D.C., Pan, G.T., Chung, S.L., Liao, Z.L., Wang, L.Q., Li, G.M., 2008. SHRIMP zircon age and geochemical constraints on the origin of lower Jurassic volcanic rocks from the Yeba Formation, southern Gangdese, south Tibet. International Geology Review 50, 442–471.
Zhu, D.C., Zhao, Z.D., Niu, Y.L., Dilek, Y., Mo, X.X., 2011a. Lhasa terrane in southern Tibet came from Australia. Geology 39, 727–730.
Zhu, D.C., Zhao, Z.D., Niu, Y.L., Mo, X.X., Chung, S.L., Hou, Z.Q., Wang, L.Q., Wu, F.Y., 2011b. The Lhasa terrane: record of a microcontinent and its histories of drift and growth. Earth and Planetary Science Letters 301, 241–255.
Zhu, D.C., Zhao, Z.D., Niu, Y.L., Dilek, Y., Hou, Z.Q., Mo, X.X., 2012. Origin and evolution of the Tibetan Plateau. Gondwana Research, http://dx.doi.org/10.1016/j.gr.2012.02.002.

Please cite this article as: Xu, W.-C., et al., Rapid Eocene erosion, sedimentation and burial in the eastern Himalayan syntaxis and its geodynamic significance, Gondwana Res. (2012), doi:10.1016/j.gr.2012.05.011